GMR Genetics and Molecular Research
Online Journal
ISSN:1676-5680

Gene expression profiling: identification of genes with altered expression in *Ayu17-449* knockout mice

Y. Li[1]*, T.T. Huang[2]*, H. Tang[2], K.I. Yamamura[3] and X.Y. Pu[1]

[1]Department of Clinical Laboratory, Xinqiao Hospital,
Third Military Medical University, Chongqing, China
[2]Key Laboratory of Molecular Biology on Infectious Diseases,
Ministry of Education, Chongqing Medical University, Chongqing, China
[3]Department of Developmental Genetics,
Institute of Molecular Embryology and Genetics, Kumamoto University,
Kumamoto, Japan

*These authors contributed equally to this study.
Corresponding author: Y. Li or H. Tang
E-mail: liyi-12qq@163.com / tanghua86162003@yahoo.com.cn

Genet. Mol. Res. 10 (3): 1533-1544 (2011)
Received January 8, 2011
Accepted Abril 10, 2011
Published August 1, 2011
DOI 10.4238/vol10-3gmr1158

ABSTRACT. *Ayu17-449*, a novel gene in mice, has been identified as a tumor-suppressor gene in myeloid malignancy; its product catalyzes the conversion of 5-methylcytosine of DNA to 5-hydroxymethylcytosine. However, *in vivo*, its functional target genes and biological function have remained unclear. Based on the assumption that alterations in the expression of the *Ayu17-449* gene affect the expression of other related genes, we screened a microarray of altered gene expression in *Ayu17-449*$^{-/-}$ and *Ayu17-449*$^{+/+}$ mice. We

identified 4049 genes with altered expression, including 1296 up-regulated (fold change ≥2) and 2753 down-regulated (fold change ≤0.5) genes in knockout mice compared with control mice. We then used qRT-PCR and RT-PCR to validate the chip data. Gene ontology and pathway analysis were performed on these altered genes. We found that these altered genes are functional genes in the complement and coagulation cascades, metabolism, biosynthesis, transcriptional regulation, proteolysis, and intracellular signaling pathways, such as the peroxisome proliferator-activated-receptor signaling pathway, the TNF-α-NF-κB pathway, the Notch signaling pathway, the MAPK signaling pathway, and the insulin signaling pathway. The results of our genome-wide comprehensive study could be helpful for comprehending the underlying functional mechanisms of the *Ayu17-449* gene in mammals.

Key words: *Ayu17-449* knockout mice; Gene microarray; *TET-2* (tet oncogene family member 2)

INTRODUCTION

Ayu17-449, a novel gene on mouse chromosome 3, was identified by the gene trapping technique previously reported by Tang et al. (2006). In NCBI database analysis, *Ayu17-449* is also called *TET-2* (tet oncogene family member 2). It belongs to a novel, well-conserved, protein family but with unclear biological function, the TET protein family, including three members (TET-1, TET-2 and TET-3). Current, related studies about the function of TET-2 were restricted to its identification as a tumor-suppressor gene commonly mutated in myeloid malignancies, including myelodysplastic syndromes (MDS; Langemeijer et al., 2009), chronic myelomonocytic leukemia (CML; Kosmider et al., 2009) or acute myeloid leukemia (AML; Nibourel et al., 2010), which may play critical roles in regulating the survival, growth and differentiation of myeloid cells. In addition, Ito et al. (2010) proved that TET-2 protein could catalyze the conversion of 5-methylcytosine (5mC) of DNA to 5-hydroxymethylcytosine (5hmC) in U2OS cells. Despite this, the function of *Ayu17-449* protein regulation mechanism in the cell physiological state remains unresolved, as does the question of whether *Ayu17-449* protein is a key factor in controlling the conversion of normal genes to tumor genes.

Gene knockout studies in rodents confirmed the central role of *Ayu17-449* in embryonic development. Tang et al. (2008) showed that in *Ayu17-449* null mice, development appears largely normal until embryonic day 19 (E19), and embryos die (at P0-P1) from unidentified causes. In adult mice, *Ayu17-449* showed a characteristic regional distribution in brain and kidney. *Ayu17-449* was identified having the granin motif, which was important for acidic granule formation in mouse proximal convoluted tubules (Tang et al., 2008). However, detailed information on the functions of granules in the proximal tubule cell was as yet unavailable. To clarify the role of *Ayu17-449* in embryonic tissue development, we used high-density oligonucleotide probe-based cDNA microarray to profile gene expression patterns of *Ayu17-449*$^{-/-}$ mouse brains at stage E19 compared to

age-matched control mouse brains, and identified the major clusters of up-regulated and down-regulated genes, which were subjected to detailed analysis.

MATERIAL AND METHODS

Animals

Heterozygous *Ayu17-449* mice (*Ayu17-449*$^{+/-}$) were produced in the Center for Animal Resources and Development, Kumamoto University, Japan, and fed in the Center of Experimental Animals, Chongqing Medical University, China. The mice were conventionally housed in polyethylene cages at a constant temperature of 22 ± 2°C, relative humidity of 55%, and on a 12-h light/dark cycle (lights on from 8:00 to 20:00). Mice were fed a standard chow diet, and food and water were provided *ad libitum*. The experimental protocols were conducted in accordance with internationally accepted principles for laboratory animal use. Five heterozygous males were mated with 10 heterozygous females to produce wild-type mice, heterozygous mice, and homozygous mice. Because the homozygous mutant mice died at P0, homozygous mice were obtained by abdominal delivery on the 19th day of pregnancy. The brain tissues of all offspring mice at E19 were taken out and immediately frozen in liquid nitrogen and then kept at -80°C until further analysis. Genotyping was done by polymerase chain reaction (PCR) analysis on tail genomic DNA.

RNA extraction and microarray hybridization

Brain samples from 3 wild-type (*Ayu17-449*$^{+/+}$) and 3 homozygous (*Ayu17-449*$^{-/-}$) mice were pooled for each genotype. Each pool was placed in 3 mL Trizol reagent (Invitrogen Corporation, Carlsbad, CA, USA) and homogenized with a homogenizer. After extraction with chloroform, RNA was precipitated with isopropanol. The resultant pellet was finally resuspended in TE buffer (10 mM Tris-HCl, pH 7.5, 1 mM EDTA). After a DNase digestion step, RNA quantification and quality assurance were assessed by optical density measurement at 260/280 nm (between 1.8 and 2.1) (Gene Quant Pro), and RNA integrity and genome DNA contamination were tested by denaturing agarose gel electrophoresis. Single-color gene-expression profiles were generated for test and control samples. These profiles were generated using customized 4 × 44 K oligonucleotide microarrays produced by Agilent Technologies (Palo Alto, CA, USA). The mouse whole-genome microarrays covered more than 41,000 genes and transcripts. The representative sequences were derived from leading public databases including RefSeq, Ensembl, Unigene, UCSC Goldenpath, and others. The RNA samples were amplified and labeled using the Agilent Quick Amp labeling kit (Agilent Technologies) according to manufacturer instructions and hybridized with the Agilent mouse whole-genome oligonucleotide microarray in Agilent's SureHyb hybridization chambers. After hybridization and washing, the hybridized slides were scanned with the Agilent DNA microarray scanner (G2505B) and processed with the Agilent Feature Extraction Analytics software (version 9.5.3). The Feature Extraction placed microarray grids, rejected outlier pixels, determined feature intensities and ratios, flagged outlier pixels, and compiled QC reports. The procedure above was carried out by KangChen Bio-Tech, Shanghai, China.

Real-time quantitative PCR (qRT-PCR) or RT-PCR

The reliability of chip results was not only confirmed by qRT-PCR analysis of the selected genes, including *Ccl4*, *Nox3*, *Gtf2h2*, *Pgam2*, *Ccr10*, and mouse β-actin gene as control, but also by RT-PCR analysis *Alb*, *Serpinalb*, *Fga*, *Serpinald*, these selected genes, and mouse GAPDH gene as control. Primer sequences for cDNA synthesis were designed by the ABI Primer Express software. The optimal annealing temperature for each primer set was determined prior to the analysis of experimental samples. Prior to RT performance, DNase I (Promega, USA) was used to digest the genomic DNA. An amount of 2 µg total RNA (the same RNA used for the arrays) from the *Ayu17-449*$^{+/+}$ or *Ayu17-449*$^{-/-}$ mice was individually subjected to reverse-transcription with random primers and a reverse transcription kit (Promega). In real-time PCR, triplicate 25-µL real-time PCRs were run, containing 12.5 µL SYBR Green PCR master mix, 1 µL of a primer stock solution containing 10 µM of both forward and reverse primers, 1 µL cDNA template, and 10.5 µL nuclease-free water. The following standard PCR conditions were used: one cycle at 90°C for 10 min and 40 cycles at 94°C for 15 s, the primer-specific annealing temperature for 40 s and 72°C for 60 s. Because different primers were used, every primer has its suitable annealing temperature, e.g., 58°, 59°, 60°C. Here, we described this process as primer-specific annealing temperature. A cycle threshold (CT) was assigned at the beginning of the logarithmic phase of PCR amplification, and duplicate CT values were analyzed by Microsoft Excel. The $2^{-\Delta\Delta Ct}$ method (Livak and Schmittgen, 2001) was used to determine the relative expression of the gene in each sample. In RT-PCR, triplicate PCR mixtures were run, containing 5 µL 5X PrimeSTAR buffer, 2 µL dNTP mixture, 2 µL of each primer (Table 1), 2 µL SureStart Taq polymerase (Takara), 1 µL cDNA template, and 13 µL nuclease-free water preparation per 25-µL reaction. The following standard PCR conditions were used: one cycle at 95°C for 10 min and 40 three-step cycles (20 s at 95°C, 30 s at 60°C, and 30 s at 72°C), and a final incubation at 72°C for 5 min. PCR products were then detected by 1.0% agarose gel electrophoresis.

Table 1. Primer sequences and product size of genes that were further tested with real-time PCR (A) and RT-PCR (B).

Gene	Product length	Forward primer	Reverse primer
A			
Ccl4	56 bp	CCCGAGCAACACCATGAAG	CCACGAGCAAGAGGAGAGAGA
Nox3	56 bp	TCTCCGGCTGCACAATGTC	CTGCCTGCCATTCAGCATAG
Gtf2h2	60 bp	GTGGCCCGAAGCGAGTT	TTTACTGTCCCCCGTGTTCAG
Pgam2	56 bp	GAGGTTCCTGGGAGACGAAGA	GGGCAGCAACAGCTTCCAT
Ccr10	60 bp	CCTCTACTCGGCCTCTTTCCA	CGGTCGGCGCTGATACAG
mβ-actin	59 bp	cga tgc cct gag gct ctt t	tgg atg cca cag gat tcc at
B			
Alb	857 bp	TTGCATGAAGTTGCCAGAAG	ACGAGAGTTGGGGTTGACAC
Serpinalb	501 bp	GGTCTACTGCTTCTGGCAGG	CACTTTCTTGGCCTCCTCTG
Fga	994 bp	CTGGCTCAGACTCTGGGAAC	TTTAAGGTTAGGGGGTTGGG
Serpinald	347 bp	AAACATCGGAGGCTGACATC	CTCAGGATCGAATGGCTGTT
Pgam2	590 bp	GCTGCCACCTAGAGTTCCTG	GGGCTGCAATAAGCACTCTC
Ccr10	371 bp	AACCCAGTGTCTCCCTGATG	CAGCCACACGAAGACTGAAA
mGAPDH	391 bp	gga aag ctg tgg cgt gat g	ctg ttg ctg tag ccg tat tc

Microarray data analysis

The Agilent GeneSpring GX software (version 7.3 or later) was used to calculate and

record the signal intensities representing the gene expression levels generated by the Agilent 4 × 44 K One-Color Whole Genome Microarray. For inter-array normalization, a median normalization was applied. For data analysis, fold changes were applied to select the differentially expressed genes using 2-fold change cutoff. Genes with 2-fold higher expression compared to control were regarded as up-regulated gene; genes with 2-fold lower expression were regarded as down-regulated genes, and 0.50- to 1.99-fold changes were regarded as non-significant. Therefore, the profiling identified a subset of the total number of differentially expressed genes. Gene ontology (GO) analysis and pathway analysis were then performed on these subsets of genes.

RESULTS

Profiling of differential gene expression in *Ayu17-449*$^{-/-}$ mice

To elucidate the mechanism of growth regulation by *Ayu17-449*, we used an *Ayu17-449* knockout mouse model described previously (Tang et al., 2008). Loss of *Ayu17-449* function in the mouse results in death around day P0 (the day of birth), but dose not appear to affect early development processes such as body axis formation (Tang et al., 2008). At embryonic stage E19, these brain tissues were taken out and microarray analysis was done for determining the distinction of gene expression between *Ayu17-449*$^{-/-}$ and *Ayu17-449*$^{+/+}$ mice. Comparison analysis revealed 1296 up-regulated genes and 2753 down-regulated genes in *Ayu17-449*$^{-/-}$ mice. The expression of *Ccl4*, *Homer1*, *Gtf2h2*, *Tubb2a*, *Xist*, *Slc22a17*, *Fxyd6*, *Snrpn*, *Ly6h*, *Adrm1*, *Arf5*, *Snurf*, *2010107G23Rik*, *BC005764*, *Mgat4b*, *2210016L21Rik*, *Tuba1b*, *Cct2*, *Podxl2*, *Ogfr*, and *Strn4* was markedly increased (Table 2), and that of *Pzp*, *Apoa1*, *Serpinc1*, *Uox*, *Igfbp1*, *Serpina1e*, *Fgg*, *Ahsg*, *Ambp*, *Hp*, *Cpb2*, *Fgb*, *F2*, *Serpina1d*, *Kng1*, *Serpina1b*, *Apoh*, *Fga*, *Fabp1*, and *Alb1* was dramatically repressed (Table 3).

Table 2. Highly up-regulated genes in *Ayu17-449*$^{-/-}$ mice in comparison with wild-type mice.

GenBank	Gene symbol	Fold change	Description
NM_013652	*Ccl4*	411.2	Chemokine (C-C motif) ligand 4
NM_011982	*Homer1*	41.45	Homer homolog 1 (*Drosophila*)
BC016231	*Gtf2h2*	25.5	General transcription factor II H, polypeptide 2
NM_009450	*Tubb2a*	18.95	Tubulin, beta 2a
L04961	*Xist*	15.4	Inactive X-specific transcripts
NM_021551	*Slc22a17*	14.44	Solute carrier family 22 (organic cation transporter), member 17
NM_022004	*Fxyd6*	14.1	FXYD domain-containing ion transport regulator 6
NM_013670	*Snrpn*	14	Small nuclear ribonucleoprotein N
NM_011837	*Ly6h*	13.61	Lymphocyte antigen 6 complex, locus H
NM_019822	*Adrm1*	13.47	Adhesion regulating molecule 1
NM_007480	*Arf5*	13.47	ADP-ribosylation factor 5
NM_033174	*Snurf*	11.92	SNRPN upstream reading frame
NM_027251	*2010107G23Rik*	11.78	RIKEN cDNA 2010107G23 gene
NM_181681	*BC005764*	11.63	cDNA sequence BC005764
NM_145926	*Mgat4b*	11.59	Mannoside acetylglucosaminyltransferase 4, isoenzyme B
NM_028211	*2210016L21Rik*	11.31	RIKEN cDNA 2210016L21 gene
NM_011654	*Tuba1b*	10.9	Tubulin, alpha 1B
NM_007636	*Cct2*	10.75	Chaperonin subunit 2 (beta)
NM_176973	*Podxl2*	10.41	Podocalyxin-like 2
NM_031373	*Ogfr*	10.26	Opioid growth factor receptor
NM_133789	*Strn4*	10.25	Striatin, calmodulin binding protein 4

Table 3. Highly down-regulated genes in *Ayu17-449*$^{-/-}$ mice in comparison with wild-type mice.

GenBank	Gene symbol	Fold change	Description
NM_007376	*Pzp*	0.000972	Pregnancy zone protein
NM_009692	*Apoa1*	0.000816	Apolipoprotein A-I
NM_080844	*Serpinc1*	0.000812	Serine (or cysteine) peptidase inhibitor, clade C (antithrombin), member 1
NM_009474	*Uox*	0.000807	Urate oxidase
NM_008341	*Igfbp1*	0.000785	Insulin-like growth factor binding protein 1
NM_009247	*Serpina1e*	0.000757	Serine (or cysteine) peptidase inhibitor, clade A, member 1e
NM_133862	*Fgg*	0.000739	Fibrinogen, gamma polypeptide
NM_013465	*Ahsg*	0.000731	Alpha-2-HS-glycoprotein
NM_007443	*Ambp*	0.000667	Alpha 1 microglobulin/bikunin
NM_017370	*Hp*	0.000618	Haptoglobin
AF186188	*Cpb2*	0.000613	Carboxypeptidase B2 (plasma)
NM_181849	*Fgb*	0.000608	Fibrinogen, B beta polypeptide
NM_010168	*F2*	0.00054	Coagulation factor II
NM_009246	*Serpina1d*	0.000502	Serine (or cysteine) peptidase inhibitor, clade A, member 1d
NM_023125	*Kng1*	0.000486	Kininogen 1
NM_009244	*Serpina1b*	0.000478	Serine (or cysteine) peptidase inhibitor, clade A, member 1b
NM_013475	*Apoh*	0.00045	Apolipoprotein H
NM_010196	*Fga*	0.000445	Fibrinogen, alpha polypeptide
NM_017399	*Fabp1*	0.000332	Fatty acid binding protein 1, liver
NM_009654	*Alb1*	0.000271	Albumin 1

Validation of microarray results by qRT-PCR or RT-PCR

To confirm the chip results, five up-regulated genes were chosen for qRT-PCR performance. The results showed that *Ccl4*, *Nox3*, *Gtf2h2*, and *Pgam2* expression patterns were similar to that observed in the microarray experiments, among which *Pgam2* mRNA expression showed no statistical significance difference between wide-type and *Ayu17-449*-deficient mice by qRT-PCR (Figure 1), but *Ccr10* was not confirmed as an up-regulated gene in *Ayu17-449*$^{-/-}$ mice by qRT-PCR or RT-PCR (data not shown), which was in opposition with microarray data (Figure 1). Meanwhile, four significantly down-regulated genes including *Alb1*, *Serpina1b*, *Fga*, and *Serpina1d* were identified by RT-PCR. These results were correlated with microarray data (Figure 2).

Bioinformatic analysis

Profiling identified a subset of the total number of probes analyzed by Agilent whole-genome oligo microarray that show differential expression. The identified differential genes were annotated in the GO format for biological function classification and in the pathway analysis format for elucidation of whole chains of events in brain tissues of *Ayu17-449*$^{-/-}$ compared with *Ayu17-449*$^{+/+}$ mice. In the GO, the identified genes including the intracellular membrane-bound organelle (P = *7.37E-16*), membrane-bound organelle (P = *7.37E-16*), mitochondrion (P = *3.27E-11*), cytoplasm (P = *1.83E-10*), and ribonucleoprotein complex (P = *7.52E-05*) were overrepresented (Figure 3). Pathway analysis revealed that, in *Ayu17-449*$^{-/-}$ mice, many pathway genes had disordered expression, especially in complement and coagulation cascades (P = *4.70E-14*), glycine, serine and threonine metabolism (P = *1.02E-07*), amino acid metabolism (P = *2.43E-07*), mRNA processing (P = *8.27E-07*), purine metabolism (P = *2.42E-05*), drug metabolism-cytochrome P450 (P = *7.61E-05*), and heme biosynthesis (P = *8.69E-05*), and so on (Table 4).

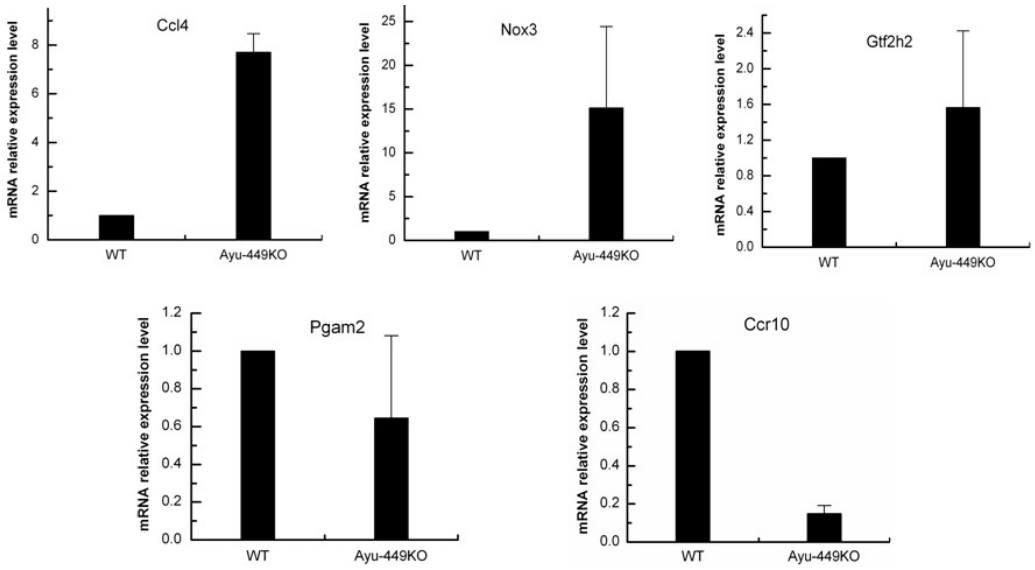

Figure 1. Validation of microarray results by real-time PCR. The results represent quantification of mRNA levels relative to β-actin. Normalized expression values obtained by real-time PCR (N = 3). WT = wild type.

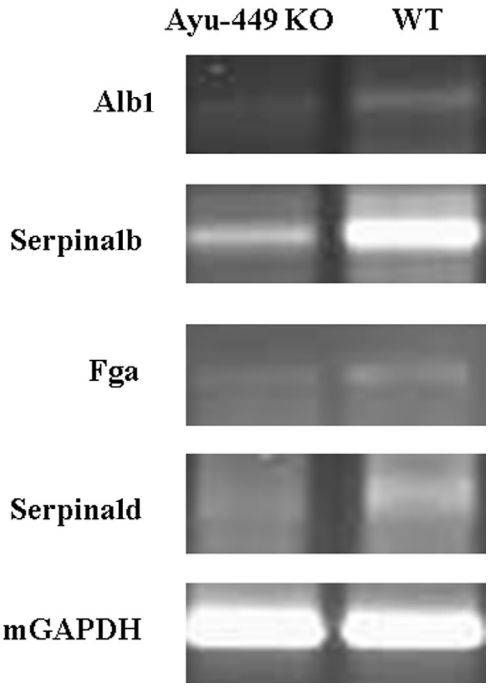

Figure 2. mRNA expression levels of altered genes in microarray validated by RT-PCR. Results show that *Alb*, *Serpinalb*, *Fga*, and *Serpinald* were down-regulated genes, using mouse GAPDH gene as an internal standard; all of which were consistent with chip data. WT = wild type.

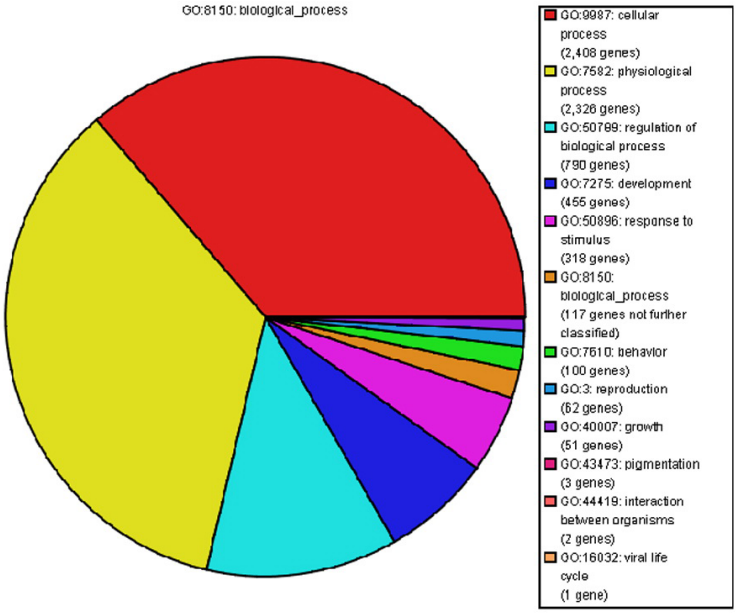

Figure 3. Gene ontology (GO) analysis used for analysis of the altered genes. Differentially expressed transcripts mapped to numerous biological processes of the hierarchical GO system. The meaning of each color representative is listed on the right side of the legend.

Table 4. Altered mRNA expression patterns of wild-type and homozygous *Ayu17-449* knockout mice over the investigated period of time (E19) as analyzed by the Pathway Analysis software.

Pathway	Number of common genes with each pathway	P value
KEGG PATHWAY: Complement and coagulation cascades - *Mus musculus* (mouse)	44	4.70E-14
KEGG PATHWAY: Glycine, serine and threonine metabolism - *Mus musculus* (mouse)	24	1.02E-07
Amino acid metabolism	38	2.43E-07
mRNA processing (*Mus musculus*)	140	8.27E-07
KEGG PATHWAY: Purine metabolism - *Mus musculus* (mouse)	49	2.42E-05
KEGG PATHWAY: Drug metabolism - cytochrome P450 - *Mus musculus* (mouse)	24	7.61E-05
Heme biosynthesis	7	8.69E-05
Statin pathway (PharmGKB)	11	0.000144
KEGG PATHWAY: PPAR signaling pathway - *Mus musculus* (mouse)	25	0.000147
Circadian exercise	22	0.00017
Fatty acid biosynthesis	12	0.000314
KEGG PATHWAY: Pyrimidine metabolism - *Mus musculus* (mouse)	30	0.000353
Blood clotting cascade	10	0.000384
TNF-alphaNF-κB signaling pathway	54	0.000399
Translation factors	22	0.000711
KEGG PATHWAY: Ribosome - *Mus musculus* (mouse)	28	0.000806
Cytoplasmic ribosomal proteins	27	0.000834
KEGG PATHWAY: Styrene degradation - *Mus musculus* (mouse)	3	0.000941

DISCUSSION

The use of gene knockout mice to study the biological function of a certain gene has

attracted much attention among many researchers (Callow et al., 2000; Monti et al., 2001; Choi et al., 2007). In our experiments, to elucidate the biological function of the novel gene *Ayu17-449*, we produced the *Ayu17-449* knockout mouse by gene trap technology (Tang et al., 2008). The finding that each *Ayu17-449*$^{-/-}$ mouse died on P0 caught our attention. In other words, once some sustaining conditions from the mother ended, some physiological defects related to *Ayu17-449* gene would have a direct lethal effect on fetal mice. We used brain tissues from E19 *Ayu17-449*$^{-/-}$ or *Ayu17-449*$^{+/+}$ mice to compare differential gene expression between them by analysis of the mouse whole-genome microarray data. We found 1296 genes (fold change ≥2) that were up-regulated and 2753 genes (fold change ≤0.5) down-regulated in *Ayu17-449*$^{-/-}$ mice. Using GO and pathway analyses, we then studied *Ayu17-449* gene function by means of exploring the physiological changes caused by *Ayu17-449*-regulated genes.

The microarray assay showed that chemokine (C-C motif) ligand 4 (*Ccl4*) was a strong up-regulated gene (fold change = 411.2) (Table 2) in *Ayu17-449*$^{-/-}$ mice, which should be suppressed by *Ayu17-449* protein in normal physiological status. As reported in a previous study, *Ccl4* acts as a critical factor in mediating inflammatory processes, promoting beneficial leukocyte recruitment to infected tissues and the clearance of the microbes (Khuu et al., 2007). However, Bless et al. (2000) demonstrated that *Ccl4* also contributed to host tissue damage associated with some inflammatory diseases. Therefore, *Ayu17-449* deficiency probably enhanced immunological damage caused by *Ccl4* overexpression. This would be an important cause of death in *Ayu17-449*$^{-/-}$ mice.

Our research revealed that *Ayu17-449* may play key roles in hematopoiesis and regulate production of some blood coagulation factors. The chip results showed that three fibrinogen genes (*Fga*, *Fgb*, *Fgg*) were extremely down-regulated. Their fold changes were 0.000445, 0.000608 and 0.000739, respectively. Fibrinogen, which is a symmetry dimer composed of three pairs of polypeptide chains termed α (or A), β (or B) and γ, is the main clot structural precursor protein and displays its function when it is enzyme-cleaved into fibrin by thrombase (Doolittle, 2003). Fibrin is an essential molecule that mediates platelet adhesion and aggregation, which are vital for the coagulation cascade (Ruggeri, 1997). In addition, our results showed that the serine (or cysteine) peptidase inhibitor, clade C (antithrombin), member 1 (*Serpinc1*) is 0.000812-fold down-regulated. Antithrombin is one of the most important serine protease inhibitors of blood coagulation; it inactivates thrombin and several serine proteases, including blood coagulation factors IXa, Xa, XIa, XIIa (Blajchman et al., 1992). All antithrombin-null mice could not survive at the 16.5 gestational days (Ishiguro et al., 2000). Serine (or cysteine) peptidase inhibitor, clade F, member 2 (*Serpinf2*) was also substantially down-regulated (0.0048-fold) in *Ayu17-449*$^{-/-}$ mice. *Serpinf2* is the principal inhibitor of plasmin and inhibits fibrinolysis and another serine (or cysteine) peptidase inhibitor with coagulation function (Aoki, 2005). Interestingly, our results revealed that factor X (*FX*), which is a major structural component of the blood clot, was also down-regulated about 0.00274-fold. *FX* can convert prothrombin to thrombin and promotes thrombus formation by activating platelets and converting fibrinogen to fibrin (Aasrum and Prydz, 2002). Moreover, some groups have proven that *FX* deficiency in mice causes partial embryonic lethality or death at birth from fatal neonatal bleeding or perinatal lethality (Dewerchin et al., 2000). Further studies are needed to determine the concrete roles that the *Ayu17-449* gene plays in precoagulation or anticoagulation.

Our results suggest that *Ayu17-449* gene could influence fetal liver function of lipid

metabolism. Alpha-2-HS-glycoprotein (*Ahsg*), fatty acid binding protein 1 (*Fabp1*), alpha-2-glycoprotein 1, zinc (*Azgp1*), angiopoietin-like 3 (*Angptl3*), hydroxysteroid (17-beta) dehydrogenase 2 (*Hsd17b2*), and carboxypeptidase N polypeptide 1 (*Cpn1*) are genes that show significant down-regulation in *Ayu17-449*$^{-/-}$ mice. *Ahsg* (fetuin) (fold change = 0.000731) is a member of the cystatin superfamily of cysteine protease inhibitors, which is an abundant serum protein in adult mammals and is expressed in many organs during embryogenesis (Terkelsen et al., 1998). *Ahsg* could act as a molecular carrier for the transportation of some insoluble molecules. It plays a significant role in promoting weight gain and insulin resistance, and may be a novel therapeutic target for type 2 diabetes mellitus, obesity or other insulin-resistant diseases (Mathews et al., 2002). *Ahsg*-null mice display the properties of high insulin sensitivity and obesity resistance (Mathews et al., 2006). Furthermore, *Ahsg* prevents extraosseous calcification induced by uremia and phosphate challenge (Westenfeld et al., 2007). Intracellular fatty acid binding proteins (*FABPs*), 0.000332-fold down-regulation compared to *Ayu17-449*$^{+/+}$ mice, are small, soluble and abundant cytoplasmic proteins. FABPs can also bind fatty acids and other small hydrophobic molecules. Although they have broad substrate specificity, they are commonly expressed in mammalian enterocytes and hepatocytes. Intracellular FABPs are considered to some degree to be involved in the process of cellular uptake, intracellular transport and esterification of long-chain fatty acids and storage and metabolism of their respective ligands, and possibly in other cellular processes, such as differentiation or regulation of gene expression (McArthur et al., 1999). Recently, loss of intestinal fatty acid binding protein was shown to increase the susceptibility of high fat diet-induced fatty liver in male mice, and it has been confirmed that *FABP* gene alteration promotes age-dependent obesity in female mice (Agellon et al., 2007; Martin et al., 2008). *Azgp*, which was down-regulated 0.00894-fold in *Ayu17-449*$^{-/-}$ mice, is a possible candidate gene for controlling weight, elucidation of polygenic inheritance, and age-dependent changes in the genetic control of obesity (Gohda et al., 2003). Angiopoietin-like protein 3 (*Angptl3*), a member of the vascular endothelial growth factor family of proteins, inhibits lipoprotein metabolism through its capacity to inhibit lipoprotein lipase (LPL) (Ge et al., 2004). LPL is known to play a central role in overall lipid metabolism and is associated with several pathophysiological conditions, such as atherosclerosis, obesity, and diabetes (Mead and Ramji, 2002). Moreover, *Angptl3* acts as an inhibitor of endothelial lipase and may be involved in the regulation of plasma high-density lipoprotein (HDL) cholesterol and HDL phospholipid levels in humans and rodents (Shimamura et al., 2007). Hydroxysteroid (17-β) dehydrogenase 2 (*HSD17B2*), another down-regulated gene (0.058472-fold) in *Ayu17-449*$^{-/-}$ mice, is vital for lipid metabolism. *HSD17B2* is a member of the aldo-keto reductase superfamily and catalyzes the conversion between 17-keto and 17β-hydroxysteroids. In addition, some HSD17B enzymes have been shown to be involved in other metabolic pathways, such as β-oxidation of fatty acids and oxidation of branched- and straight-chain fatty acids (Baes et al., 2000).

Knockout *Ayu17-449* gene would decrease the expression of key signal transduction pathway-related genes, for instance, *HSD17B2* (fold change = 0.00881), angiotensinogen (fold change = 0.31), Mn superoxide dismutase (*Sod2*) (fold change = 0.358), SMAD family member 5 (*Smad5*) (fold change = 0.392), potassium inwardly-rectifying channel, subfamily J, member 8 (*KCNJ8*) (fold change = 0.397), 3 beta-hydroxysterol-delta(24)-reductase (*DHCR24*) (fold change = 0.484). These genes play very importance roles in maintaining the normal survival status. Homozygous *HSD17B2* knockout mice would result in embryonic

lethality (Rantakari et al., 2008). Gene knockout of the *KCNJ8*-encoded Kir6.1 K_{ATP} channel is predisposed to an early and profound survival disadvantage (Kane et al., 2006). Targeted disruption of *DHCR24*, an enzyme catalyzing the conversion of desmosterol to cholesterol, caused death in mice within a few hours after birth (Mirza et al., 2006). Angiotensinogen-gene knockout mice are not able to restore blood pressure and sodium-water depletion to normal levels, and about 60% do not survive until weaning (Umemura et al., 1998). Tsan et al. (1998) have shown that homozygous Mn superoxide dismutase (*Sod2*) gene-knockout mice (*Sod2*$^{-/-}$) die shortly after birth with extensive myocardial injury. Smad5 has been implicated as a downstream signal mediator for several bone morphogenetic proteins. Homozygous mutant embryos die between E9.5 and E11.5, and display variable phenotypes (Chang et al., 1999). The *Smad2* gene knockout mice were independently researched by three groups. Although different strategies were used, all mutant mice died during the early stage of embryonic development, indicating that Smad2-mediated TGF-β signals are required for the early development of embryos (Nomura and Li, 1998; Waldrip et al., 1998; Weinstein et al., 1998).

The results of this study are completely from the whole genome microarray data comparing *Ayu17-449* knockout and wild-type mice. They reveal that *Ayu17-449* regulates the expression of several important genes involved in complement and coagulation cascade, complement activity, metabolism and cell differentiation, proliferation, and apoptosis. These data only provide a road map for future studies, a great deal of research is needed to understand the true biological activities of *Ayu17-449* gene, by gene addition, protein-protein interaction or other methods.

ACKNOWLEDGMENTS

Research supported by the Nature Science Foundation of China (#30671080).

REFERENCES

Aasrum M and Prydz H (2002). Gene targeting of tissue factor, factor X, and factor VII in mice: their involvement in embryonic development. *Biochemistry (Mosc.)* 67: 25-32.

Agellon LB, Drozdowski L, Li L, Iordache C, et al. (2007). Loss of intestinal fatty acid binding protein increases the susceptibility of male mice to high fat diet-induced fatty liver. *Biochim. Biophys. Acta* 1771: 1283-1288.

Aoki N (2005). The past, present and future of plasmin inhibitor. *Thromb. Res.* 116: 455-464.

Baes M, Huyghe S, Carmeliet P, Declercq PE, et al. (2000). Inactivation of the peroxisomal multifunctional protein-2 in mice impedes the degradation of not only 2-methyl-branched fatty acids and bile acid intermediates but also of very long chain fatty acids. *J. Biol. Chem.* 275: 16329-16336.

Blajchman MA, Austin RC, Fernandez-Rachubinski F and Sheffield WP (1992). Molecular basis of inherited human antithrombin deficiency. *Blood* 80: 2159-2171.

Bless NM, Huber-Lang M, Guo RF, Warner RL, et al. (2000). Role of CC chemokines (macrophage inflammatory protein-1 beta, monocyte chemoattractant protein-1, RANTES) in acute lung injury in rats. *J. Immunol.* 164: 2650-2659.

Callow MJ, Dudoit S, Gong EL, Speed TP, et al. (2000). Microarray expression profiling identifies genes with altered expression in HDL-deficient mice. *Genome Res.* 10: 2022-2029.

Chang H, Huylebroeck D, Verschueren K, Guo Q, et al. (1999). Smad5 knockout mice die at mid-gestation due to multiple embryonic and extraembryonic defects. *Development* 126: 1631-1642.

Choi Y, Qin Y, Berger MF, Ballow DJ, et al. (2007). Microarray analyses of newborn mouse ovaries lacking Nobox. *Biol. Reprod.* 77: 312-319.

Dewerchin M, Liang Z, Moons L, Carmeliet P, et al. (2000). Blood coagulation factor X deficiency causes partial embryonic lethality and fatal neonatal bleeding in mice. *Thromb. Haemost.* 83: 185-190.

Doolittle RF (2003). X-ray crystallographic studies on fibrinogen and fibrin. *J. Thromb. Haemost.* 1: 1559-1565.

Ge H, Yang G, Yu X, Pourbahrami T, et al. (2004). Oligomerization state-dependent hyperlipidemic effect of angiopoietin-like protein 4. *J. Lipid Res.* 45: 2071-2079.

Gohda T, Makita Y, Shike T, Tanimoto M, et al. (2003). Identification of epistatic interaction involved in obesity using the KK/Ta mouse as a Type 2 diabetes model: is Zn-alpha2 glycoprotein-1 a candidate gene for obesity? *Diabetes* 52: 2175-2181.

Ishiguro K, Kojima T, Kadomatsu K, Nakayama Y, et al. (2000). Complete antithrombin deficiency in mice results in embryonic lethality. *J. Clin. Invest* 106: 873-878.

Ito S, D'Alessio AC, Taranova OV, Hong K, et al. (2010). Role of Tet proteins in 5mC to 5hmC conversion, ES-cell self-renewal and inner cell mass specification. *Nature* 466: 1129-1133.

Kane GC, Lam CF, O'Cochlain F, Hodgson DM, et al. (2006). Gene knockout of the KCNJ8-encoded Kir6.1 K(ATP) channel imparts fatal susceptibility to endotoxemia. *FASEB J.* 20: 2271-2280.

Khuu CH, Barrozo RM, Hai T and Weinstein SL (2007). Activating transcription factor 3 (ATF3) represses the expression of CCL4 in murine macrophages. *Mol. Immunol.* 44: 1598-1605.

Kosmider O, Gelsi-Boyer V, Ciudad M, Racoeur C, et al. (2009). TET2 gene mutation is a frequent and adverse event in chronic myelomonocytic leukemia. *Haematologica* 94: 1676-1681.

Langemeijer SM, Kuiper RP, Berends M, Knops R, et al. (2009). Acquired mutations in TET2 are common in myelodysplastic syndromes. *Nat. Genet.* 41: 838-842.

Livak KJ and Schmittgen TD. (2001). Analysis of relative gene expression data using real-time quantitative PCR and the $2^{-\Delta\Delta CT}$ method. *Methods* 25: 402-408.

Martin GG, Atshaves BP, McIntosh AL, Mackie JT, et al. (2008). Liver fatty acid-binding protein gene-ablated female mice exhibit increased age-dependent obesity. *J. Nutr.* 138: 1859-1865.

Mathews ST, Singh GP, Ranalletta M, Cintron VJ, et al. (2002). Improved insulin sensitivity and resistance to weight gain in mice null for the Ahsg gene. *Diabetes* 51: 2450-2458.

Mathews ST, Rakhade S, Zhou X, Parker GC, et al. (2006). Fetuin-null mice are protected against obesity and insulin resistance associated with aging. *Biochem. Biophys. Res. Commun.* 350: 437-443.

McArthur MJ, Atshaves BP, Frolov A, Foxworth WD, et al. (1999). Cellular uptake and intracellular trafficking of long chain fatty acids. *J. Lipid Res.* 40: 1371-1383.

Mead JR and Ramji DP (2002). The pivotal role of lipoprotein lipase in atherosclerosis. *Cardiovasc. Res.* 55: 261-269.

Mirza R, Hayasaka S, Takagishi Y, Kambe F, et al. (2006). DHCR24 gene knockout mice demonstrate lethal dermopathy with differentiation and maturation defects in the epidermis. *J. Invest. Dermatol.* 126: 638-647.

Monti J, Gross V, Luft FC, Franca MA, et al. (2001). Expression analysis using oligonucleotide microarrays in mice lacking bradykinin type 2 receptors. *Hypertension* 38: E1-E3.

Nibourel O, Kosmider O, Cheok M, Boissel N, et al. (2010). Incidence and prognostic value of TET2 alterations in de novo acute myeloid leukemia achieving complete remission. *Blood* 116: 1132-1135.

Nomura M and Li E (1998). Smad2 role in mesoderm formation, left-right patterning and craniofacial development. *Nature* 393: 786-790.

Rantakari P, Strauss L, Kiviranta R, Lagerbohm H, et al. (2008). Placenta defects and embryonic lethality resulting from disruption of mouse hydroxysteroid (17-beta) dehydrogenase 2 gene. *Mol. Endocrinol.* 22: 665-675.

Ruggeri ZM (1997). Mechanisms initiating platelet thrombus formation. *Thromb. Haemost.* 78: 611-616.

Shimamura M, Matsuda M, Yasumo H, Okazaki M, et al. (2007). Angiopoietin-like protein3 regulates plasma HDL cholesterol through suppression of endothelial lipase. *Arterioscler. Thromb. Vasc. Biol.* 27: 366-372.

Tang H, Araki K and Yamamura K (2006). Cloning and expression analysis of a murine novel gene, Ayu17-449. *Yi. Chuan Xue Bao.* 33: 413-419.

Tang H, Araki K, Li Z and Yamamura K (2008). Characterization of Ayu17-449 gene expression and resultant kidney pathology in a knockout mouse model. *Transgenic Res.* 17: 599-608.

Terkelsen OB, Jahnen-Dechent W, Nielsen H, Moos T, et al. (1998). Rat fetuin: distribution of protein and mRNA in embryonic and neonatal rat tissues. *Anat. Embryol. (Berl)* 197: 125-133.

Tsan MF, White JE, Caska B, Epstein CJ, et al. (1998). Susceptibility of heterozygous MnSOD gene-knockout mice to oxygen toxicity. *Am. J. Respir. Cell Mol. Biol.* 19: 114-120.

Umemura S, Kihara M, Sumida Y, Yabana M, et al. (1998). Endocrinological abnormalities in angiotensinogen-gene knockout mice: studies of hormonal responses to dietary salt loading. *J. Hypertens.* 16: 285-289.

Waldrip WR, Bikoff EK, Hoodless PA, Wrana JL, et al. (1998). Smad2 signaling in extraembryonic tissues determines anterior-posterior polarity of the early mouse embryo. *Cell* 92: 797-808.

Weinstein M, Yang X, Li C, Xu X, et al. (1998). Failure of egg cylinder elongation and mesoderm induction in mouse embryos lacking the tumor suppressor smad2. *Proc. Natl. Acad. Sci. U. S. A.* 95: 9378-9383.

Westenfeld R, Schafer C, Smeets R, Brandenburg VM, et al. (2007). Fetuin-A (AHSG) prevents extraosseous calcification induced by uraemia and phosphate challenge in mice. *Nephrol. Dial. Transplant.* 22: 1537-1546.